

Figure 1: One-funneled torus with Fenchel–Nielsen coordinates: a pair of shortest geodesic γ_1 , γ_2 and angle inbetween φ . Artistic impression. There is no embedding into \mathbb{R}^3 .

A Heuristic analysis of symmetric tori

A.1 Introduction: plots of zeros and conjectures

In this part we apply ideas developed in [7] to study the Selberg zeta function associated to a symmetric one-holed torus. The Selberg zeta function corresponding to the holed torus would be the same as the one associated to a genus one hyperbolic surface with a single funnel, the case studied by D. Borthwick and T. Weich [2], [3].

As before, we start with numerical experiments. It is well-known that as a Riemann surface a one-holed torus is uniquely defined by the length of two shortest geodesics and the angle in between as shown in Figure 1. We say that a one holed torus is symmetric if the two geodesic have the same length and orthogonal to each other. Therefore a symmetric one-holed torus has only one parameter and we will denote it by $\mathring{\mathbb{T}}(a)$. We would like to consider three different symmetric tori¹ $\mathring{\mathbb{T}}(10)$, $\mathring{\mathbb{T}}(14 \log 2 + 0.05)$, and $\mathring{\mathbb{T}}(14 \log 2)$.

It is known [6] that the width of the critical strip is proportional to the reciprocal of the length of the shortest closed geodesic. Physical dimensions of paper and screen impose limitations on the figures. To make them more realistic, we plot rescaled zeros and chose proportions of the image to fit the scale on the axis. In addition, the algorithm we are using allows to compute the zeros in a small part of the critical strip near the real axis $0 < \Re s < \delta$, $0 < \Im s < e^{\frac{3a}{2}}$ only. We refer to this subset of the zero set as “small zeros”, and these are *the only zeros we consider here*, unless stated otherwise.

Three sample plots are shown in Figure 2. The plot in Figure 2(b) corresponds to a small region of the plot in [4], p. 30, Fig. 7 (bottom) near the imaginary axis, and the plot in Figure 2(c) corresponds to the plot in [2], p. 7, Fig. 11 (left).

¹This choice will be clear later, here we just note that the first choice $a = 10$ is guided by previous research [2] and the integer part $\left\lceil \frac{10}{\log 2} \right\rceil = 14$.

We will be using the following notation. Let

$$\widehat{\mathcal{Z}}(a) \stackrel{\text{def}}{=} \left\{ \hat{z} = a(\Re z + e^{-2a}\Im z) \mid \zeta_{\mathring{\mathbb{T}}(a)}(z) = 0, 0 < \Im z < e^{\frac{3a}{2}} \right\} \quad (1)$$

be a set of small rescaled zeros of the Ruelle zeta function $\zeta_{\mathring{\mathbb{T}}(a)}$ associated to the torus $\mathring{\mathbb{T}}(a)$.

Based on numerical experiments we state several conjectures on properties of small rescaled zeros, which we will try to explain heuristically in Section §A.4, leaving rigorous arguments for another occasion.

To characterise the density of the set of small zeros we introduce a cover by open balls

$$Cr(\widehat{\mathcal{Z}}) = \bigcup_{z \in \widehat{\mathcal{Z}}} B(z, r(z)), \text{ where } r(z) = \min_{z' \neq z, z' \in \widehat{\mathcal{Z}}} |z - z'|. \quad (2)$$

The plots illustrating the cover in the cases which we consider are shown in Figure 3.

In order to describe differences between the sets of small rescaled zeros corresponding to different tori, we will study the dependence of the following characteristics on the length parameter a .

1. The Hausdorff distance between the convex hull of the set of small rescaled zeros and the set itself $D_H(a) \stackrel{\text{def}}{=} \text{dist}_H(\text{Conv}(\widehat{\mathcal{Z}}(a)), \widehat{\mathcal{Z}}(a))$;
2. The area of the cover $M(a) \stackrel{\text{def}}{=} \text{Area}(Cr(\widehat{\mathcal{Z}}(a)))$;
3. Expectation $E(a) \stackrel{\text{def}}{=} \mathbb{E}(\inf |z - \widehat{\mathcal{Z}}(a)|)$ and variance $V(a) = \text{Var}(\inf |z - \widehat{\mathcal{Z}}(a)|)$ of the distance from a randomly chosen point z in the critical strip to $\widehat{\mathcal{Z}}(a)$.

Our empirical results are presented in Table 1 and is a basis for the following conjecture.

Conjecture 1 (distribution of rescaled zeros near the real axis). The Hausdorff distance D_H , the area function M , the expectation E , and the variance V are continuous and monotone functions with respect to the fractional part $\left\{ \frac{a}{\log 2} \right\}$. In particular, D_H and M are increasing while E and V are decreasing. Therefore, $a \in \mathbb{N} \log 2$ are local maxima for E and V , and local minima for D_H and M .

In the case of $\mathring{\mathbb{T}}(k \log 2)$ for some $k \in \mathbb{N}$ small zeros can be described more precisely.

Conjecture 2 (the case of rationally-dependent short geodesics). Let $a \in \mathbb{N} \log 2$. Small zeros with $0 < \Im z \leq e^{\frac{3a}{2}}$ lie on a small number of well defined lines. Among them, there are $\frac{a}{\log 2}$ lines nearly parallel to the imaginary axis if $\frac{a}{\log 2}$ is odd, and $\frac{a}{2 \log 2}$ lines nearly parallel to the imaginary axis if $\frac{a}{\log 2}$ is even.

The following conjecture address properties of the non-rescaled zero set of $\zeta_{\mathring{\mathbb{T}}(a)}$ independent of number-theoretic properties of a .

Table 1: Hausdorff distance, expectation, variance, and area of the cover.

$\left\{\frac{a}{\log 2}\right\}$	$D_H(a)$	$M(a)$	$E(a)$	$V(a)$
0	0.1671 ...	0.130210 ...	0.040 ...	0.001 ...
0.072 ...	0.0356 ...	0.901338 ...	0.010 ...	$10^{-5} \cdot 5.1 ...$
0.427 ...	0.0041 ...	1.060217 ...	0.006 ...	$10^{-6} \cdot 9.6 ...$

Table 2: Dispersion and expectation of the distance to the zero set measured using different choices of sample points.

Sample point distribution	Expectation	Dispersion
Symmetric torus $a = 14 \log 2$		
regular rectangular 100×50000 points	0.040454 ...	0.001345 ...
random 50×1000 points	0.040417 ...	0.001347 ...
random 100×50000 points	0.040361 ...	0.001347 ...
Symmetric torus $a = 14 \log 2 + 0.05$		
regular rectangular 100×50000 points	0.010254 ...	$10^{-5} \cdot 5.135236 ...$
random 50×1000 points	0.010212 ...	$10^{-5} \cdot 5.163147 ...$
random 100×50000 points	0.010218 ...	$10^{-5} \cdot 5.148808 ...$
Symmetric torus $a = 10 = 14 \log 2 + 0.29 ...$		
regular rectangular 100×50000 points	0.005994 ...	$10^{-6} \cdot 9.705229 ...$
random 50×1000 points	0.006002 ...	$10^{-6} \cdot 9.641849 ...$
random 100×50000 points	0.005972 ...	$10^{-6} \cdot 9.657625 ...$

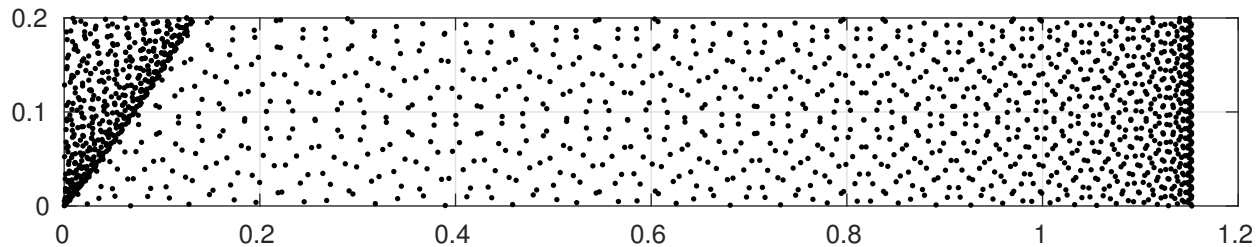
Conjecture 3 (distribution of zeros on a large scale). The zero set of the Selberg zeta function for $\mathring{\mathbb{T}}(a)$ has the following properties

1. The asymptotic of the number of zeros in the critical strip with $\Im z < t$ is

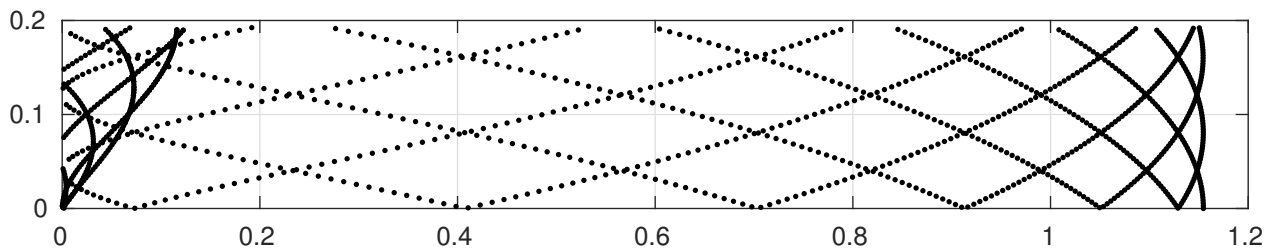
$$\#\{z \in \mathbb{C} \mid 0 < \Re z < \delta, 0 < \Im z < t, \zeta_{\mathring{\mathbb{T}}(a)}(z) = 0\} = \frac{2a}{\pi}t + O(1);$$

2. Any rectangle in the critical strip of the height $\frac{\pi}{a}$ contains at least one zero;
3. The real parts of zeros are dense in $(0, \frac{1}{2}\delta)$.

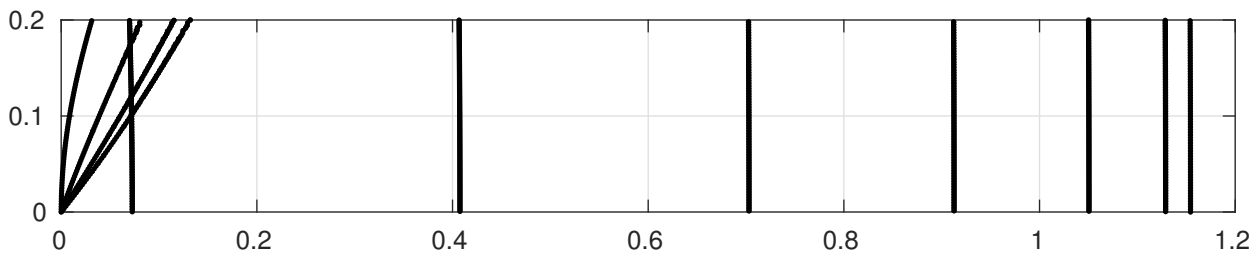
Figure 2: Characteristic plots of rescaled zeros of symmetric torus. Larger balls mean that the rescaled zeros are further away.



(a) The plot shows 1777 rescaled zeros $z \in \widehat{\mathcal{Z}}(10)$, $0 < \Im z < 0.2$.

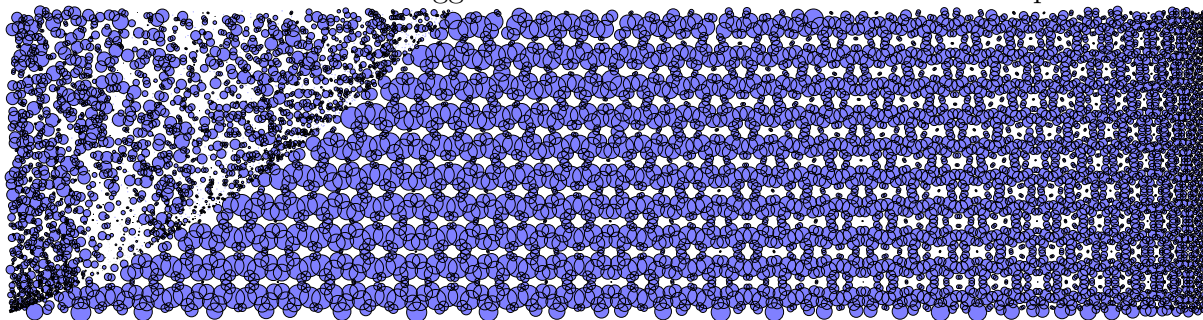


(b) The plot shows 1382 rescaled zeros $z \in \widehat{\mathcal{Z}}(14 \log 2 + 0.05)$, $0 < \Im z < 0.2$.

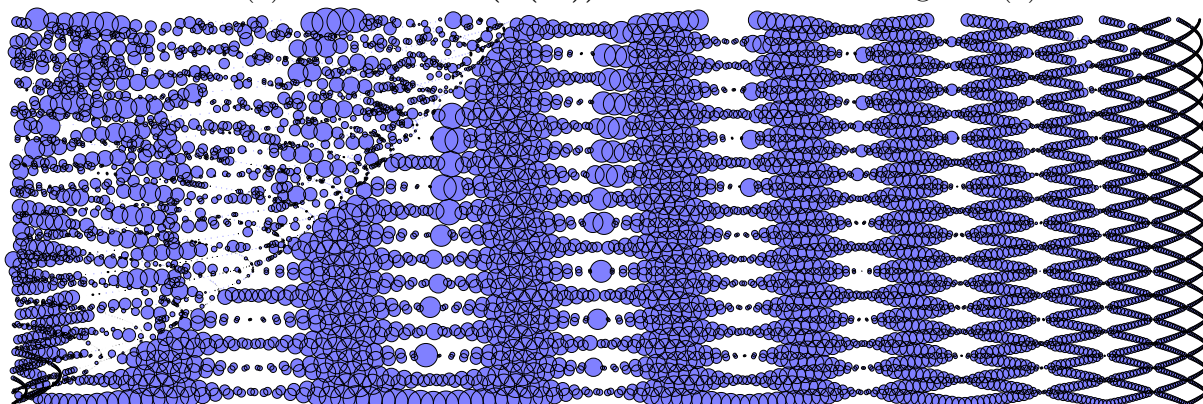


(c) The plot shows 1359 rescaled zeros $z \in \widehat{\mathcal{Z}}(14 \log 2)$, $0 < \Im z < 0.2$.

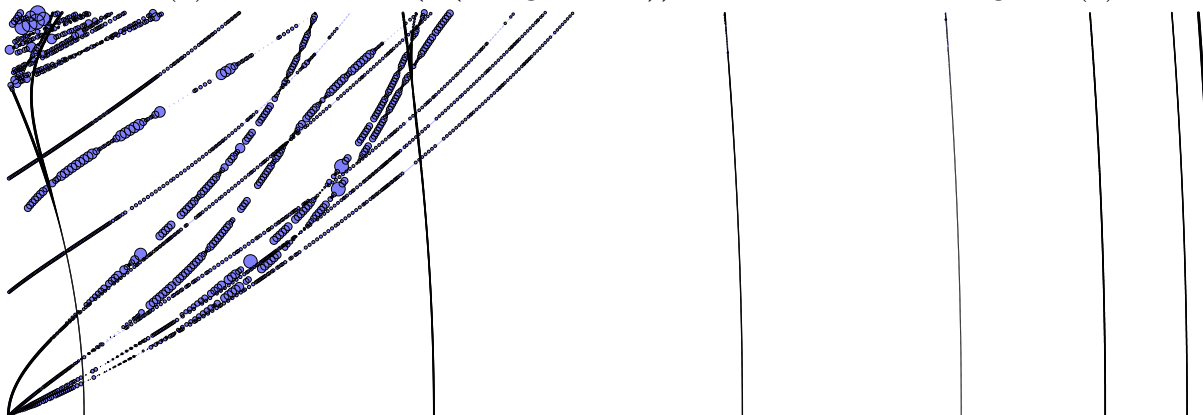
Figure 3: Characteristic plots of rescaled zeros with a cover by disks of the radius equal to the distance to the nearest zero. Bigger disks mean that the zeros are further apart.



(a) The cover $Cr(\widehat{Z}(10))$ of the zero set from Figure 2(a).



(b) The cover $Cr(\widehat{Z}(14 \log 2 + 0.05))$ of the zero set from Figure 2(b).



(c) The cover $Cr(\widehat{Z}(14 \log 2))$ of the zero set from Figure 2(c).

A.2 Geometry of a one-holed torus

A very good exposition can be found in Buser and Semmler [5]. Here we summarise the results we need making necessary adaptations to the case we consider. A one holed torus is a genus one Riemann surface whose boundary consists of a single simple closed geodesic. In order to estimate the length of the closed geodesics we use Fenchel—Nielsen coordinates and a universal cover by a holed plane. It turns out that in the case of symmetric one-holed torus the universal cover has one parameter. Namely, we may consider a right-angled hyperbolic pentagon with the sides $\{a, *, b, *, a\}$ as shown by the shaded area in Figure 4(a). It is known cf. [1], §7.18 that a and b satisfy the identity

$$\sinh^2 a = \cosh b.$$

Fixing the length of the boundary geodesic b we compute

$$a = \frac{1}{2} \ln \left(e^b + e^{-b} + 1 + \sqrt{e^{2b} + e^{-2b} + 2(e^b + e^{-b}) + 1} \right) = \frac{1}{2} \left(b + \log 2 + e^{-b} + \frac{1}{3} e^{-3b} + o(e^{-3b}) \right). \quad (3)$$

We can glue together four identical pentagons Q and obtain a hyperbolic right-angled octagon \tilde{Q} as shown in Figure 4(a). The octagon is uniquely determined up to an isometry by b , which can vary freely in $(0, +\infty)$.

For visualisation purposes, consider the octagon \tilde{Q} as an ordinary right-angled octagon on \mathbb{R}^2 plane, with four quarters of a circle as alternating sides and other four sides parallel to coordinate axis. We assign labels ∇ and \triangle to two sides parallel to the horizontal axis and \triangleright and \triangleleft to the sides parallel to the vertical axis. Translating the octagon along vertical and horizontal axes we obtain a tessellation of a holed plane Ω , where the holes are Euclidean disks made of four quarters of the boundary circles glued together, as shown in Figure 4(b). The holed plane Ω is a universal cover of a symmetric one-holed torus, and carries the hyperbolic structure of \tilde{Q} . Evidently there is a natural action of the group $\Gamma = \mathbb{Z} \times \mathbb{Z}$ on Ω by isometries and copies $\tilde{Q}_{i,j}$ of \tilde{Q} are fundamental domains. Two dashed lines in \tilde{Q} give a pair of shortest closed geodesics in Ω/Γ , which are generators of the fundamental group.

We can use the isometry between the plane and the torus with hyperbolic metric in order to estimate the lengths of closed geodesics.

It is known that every closed oriented geodesic γ on Ω/Γ is freely homotopic to a periodic word $\dots \triangle^{n_1} \triangleright^{k_1} \triangle^{n_2} \triangleright^{k_2} \dots \triangle^{n_t} \triangleright^{k_t} \dots$ of period $\omega(\gamma) \stackrel{\text{def}}{=} |n_1| + \dots + |n_t| + |k_1| + \dots + |k_t|$ where n_j and k_j are integers and $\triangleleft = \triangleright^{-1}$, $\triangle = \nabla^{-1}$. We denote this geodesic by

$$\gamma_{(\triangle^{n_1} \triangleright^{k_1} \triangle^{n_2} \triangleright^{k_2} \dots \triangle^{n_t} \triangleright^{k_t})},$$

and we call the periodic sequence $(\triangle^{n_1} \triangleright^{k_1} \triangle^{n_2} \triangleright^{k_2} \dots \triangle^{n_t} \triangleright^{k_t})$ the cutting sequence associated to the closed geodesics. A good exposition on cutting sequences associated to closed geodesics on a one-holed torus can be found in [8].

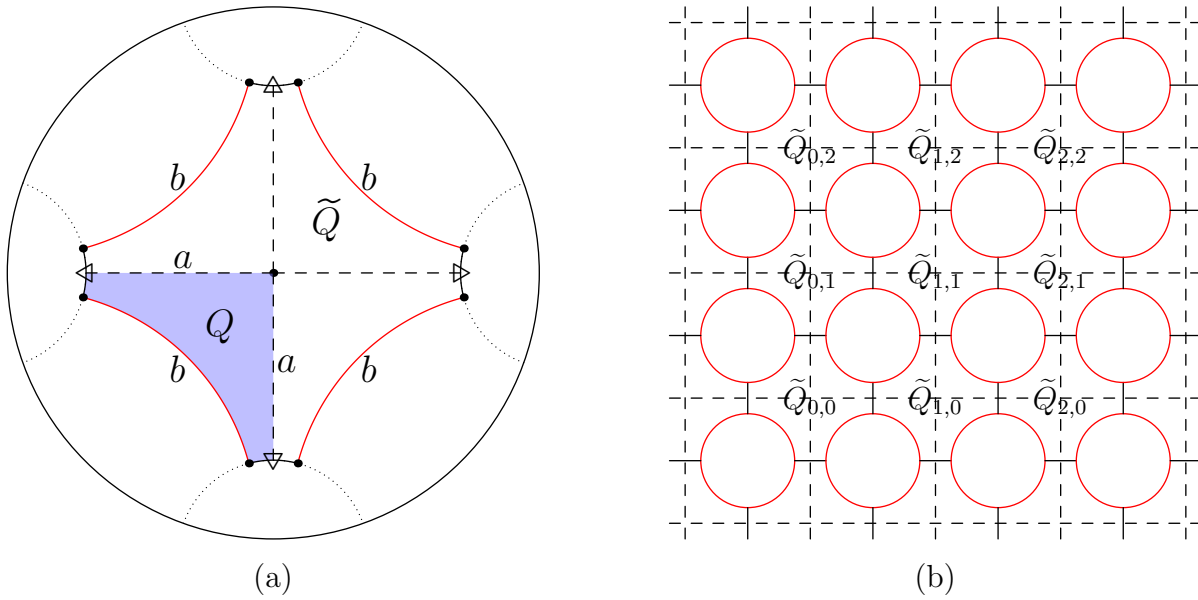


Figure 4: (a) A right-angled hyperbolic pentagon Q and its three copies forming a fundamental domain \tilde{Q} in the Poincaré disk. (b) A tessellation of $\mathbb{Z} \times \mathbb{Z}$ -holed real plane by copies of the fundamental domain $\tilde{Q}_{i,j}$.

The homotopy is unique up to conjugation by fundamental group. In particular, the two shortest geodesics correspond to the “constant” sequences of period one (\triangleright) and (\triangledown).

The homotopy defines a bijection between periodic two-sided infinite sequences $\{\sigma_k\}_{-\infty}^{\infty}$ in the alphabet $\Sigma = \{\Delta, \nabla, \triangleright, \triangleleft\}$ which satisfy an additional condition that $\sigma_k \neq \sigma_{k+1}^{-1}$ for any $k \in \mathbb{Z}$. We define a transition matrix

$$\mathbb{A} = \begin{pmatrix} 1 & 0 & 1 & 1 \\ 0 & 1 & 1 & 1 \\ 1 & 1 & 1 & 0 \\ 1 & 1 & 0 & 1 \end{pmatrix}.$$

Let $\Sigma^{\mathbb{A}}$ be the set of words which are freely homotopic to geodesics on Ω/Γ , and periodic words in $\Sigma^{\mathbb{A}}$ correspond to closed geodesics. The shift on $\Sigma^{\mathbb{A}}$ corresponds to action of Γ on closed geodesics.

It is easier to do the calculations using the upper half model $H = \{z \in \mathbb{C} \mid \Im z > 0\}$ of the hyperbolic plane and a subgroup of $PSL(2, \mathbb{R})$ acting on H . Namely, consider matrices

$$B = \begin{pmatrix} \cosh(a) & -\sinh(a) \\ -\sinh(a) & \cosh(a) \end{pmatrix} \quad C = \begin{pmatrix} e^a & 0 \\ 0 & e^{-a} \end{pmatrix}$$

Then the subgroup $\langle B, C \rangle \subset PSL(2, \mathbb{R})$ is a deck group of the universal cover $H \rightarrow \Omega/\Gamma$ and generators B and C correspond to the generators $\gamma_{(\triangledown)}$ and $\gamma_{(\triangleright)}$ of the fundamental group

of Ω/Γ . Moreover, the hyperbolic length of the geodesic corresponding to the cutting sequence $\dots \triangle^{n_1} \triangleright^{k_1} \triangle^{n_2} \triangleright^{k_2} \dots \triangle^{n_t} \triangleright^{k_t} \dots$ of period $\omega(\gamma) \stackrel{\text{def}}{=} |n_1| + \dots + |n_t| + |k_1| + \dots + |k_t|$, (where $k_j \neq 0$, $n_j \neq 0$ for $j = 1, \dots, t$) is given by

$$\ell(\gamma_{(\triangle^{n_1} \triangleright^{k_1} \triangle^{n_2} \triangleright^{k_2} \dots \triangle^{n_t} \triangleright^{k_t})}) = 2 \operatorname{ArcCosh} \left(\frac{1}{2} \left| \operatorname{tr} (B^{n_1} C^{k_1} B^{n_2} C^{k_2} \dots B^{n_t} C^{k_t}) \right| \right). \quad (4)$$

A.3 Approximating determinant

Notation 1. Given a subsequence $\sigma_1, \dots, \sigma_k$ of a sequence $\sigma \in \Sigma^{\mathbb{A}}$ we denote by $\gamma_{\sigma_1, \dots, \sigma_k}$ a geodesic whose cutting sequence contains the subsequence $\sigma_1, \dots, \sigma_k$. We denote by $\gamma_{[\sigma_1, \dots, \sigma_k]}$ a segment of a geodesic whose cutting sequence contains a subsequence $\sigma_1, \dots, \sigma_k$ with end points in the middle of the segments enclosed between intersections with the sides σ_1, σ_2 and σ_{k-1}, σ_k . We denote by $\underline{\gamma}_{[\sigma_1, \dots, \sigma_k]}$ the segment of the shortest of all closed geodesics whose cutting sequence contains the subsequence $\sigma_1, \dots, \sigma_k$ with end points in the middle of segments enclosed between intersections with the sides labelled σ_1, σ_2 and σ_{k-1}, σ_k , respectively. Then $\ell(\underline{\gamma}_{[\sigma_1, \dots, \sigma_k]}) = \ell(\gamma_{[\sigma_1, \dots, \sigma_k]})$, where γ is a primitive closed geodesic such that $\ell(\gamma) = \min_{\gamma'} \{ \ell(\gamma') \mid \gamma' \text{ intersects } \sigma_1, \dots, \sigma_k \}$.

Let $\sigma^1, \dots, \sigma^N$ be all subsequences of sequences $\sigma \in \Sigma^{\mathbb{A}}$ of the length n . Let us consider an $N \times N$ transition matrix given by

$$\mathbb{A}_{i,j}^n = \begin{cases} 1, & \text{if } \sigma_{k+1}^i = \sigma_k^j; \text{ for } k = 1, 2, \dots, n-1. \\ 0, & \text{otherwise.} \end{cases}$$

We now define a one-parameter family of $N \times N$ matrices $A(s)$ which elements depend on the length of geodesic segments determined by σ^i and σ^j :

$$A: \mathbb{C} \rightarrow \operatorname{Mat}(N \times N) \quad A_{i,j}(s) = \mathbb{A}_{i,j}^n \cdot \exp(-s \cdot \ell(\gamma_{[\sigma_1^i \sigma_2^j \dots \sigma_n^i \sigma_n^j]})) \quad (5)$$

Note that A depends on n , but we omit this in the notation. We will be using the following Lemma from [7] to find approximate location of the zeros.

Lemma 1. *Using the notation introduced above, we have the following representation for the Ruelle zeta function*

$$\zeta_X(s) = \prod_{n=0}^{\infty} \prod_{\substack{\gamma=\text{primitive} \\ \text{closed geodesic}}} (1 - e^{-(s+n)\ell(\gamma)}) = \lim_{n \rightarrow \infty} \det(\operatorname{Id}_n - A(s)), \quad (6)$$

where $\operatorname{Id}_n \in \operatorname{Mat}(n, n)$ is the identity matrix.

Our first Lemma gives approximations to lengths of geodesic segments.

Lemma 2.

$$\ell(\underline{\gamma_{[\nabla\nabla\nabla]}}) = 2a - \log \sqrt{2} + o(e^{-3a}) \quad \text{see Figure 6(b);} \quad (7)$$

$$\ell(\underline{\gamma_{[\Delta\nabla\Delta]}}) = 2a - \log 2 - 2e^{-2a} + o(e^{-3a}) \quad \text{see Figure 6(b);} \quad (8)$$

$$\ell(\underline{\gamma_{[\Delta\nabla\nabla]}}) = 2a - \log 2 + 2e^{-2a} + o(e^{-3a}) \quad \text{see Figure 5(b).} \quad (9)$$

Proof. The result follows by straightforward calculation by applying formula (4) together with (3) to $\gamma_{(\Delta\nabla\nabla)}$, $\gamma_{(\nabla\nabla\nabla)}$, and $\gamma_{(\Delta\nabla\Delta)}$, respectively. More precisely, by definition we have that

$$\begin{aligned} \ell(\underline{\gamma_{[\Delta\nabla\nabla]}}) &= \frac{1}{4}\ell(\gamma_{(\Delta\nabla\nabla)}) = \frac{1}{2} \text{ArcCosh} \left(\frac{1}{2} |\text{tr}(B^{-1}CBC^{-1})| \right) = \\ &= \frac{1}{2} \text{ArcCosh} \left(-\frac{e^{4a} + e^{-4a}}{8} + \frac{e^{2a} + e^{-2a}}{2} + \frac{1}{4} \right) = 2a - \log 2 - 2e^{-2a} - 5e^{-4a} + o(e^{-4a}). \end{aligned} \quad (10)$$

Similarly,

$$\begin{aligned} \ell(\underline{\gamma_{[\nabla\nabla\nabla]}}) &= \frac{1}{4}\ell(\gamma_{(\nabla\nabla\nabla)}) = \frac{1}{2} \text{ArcCosh} \left(\frac{1}{2} |\text{tr}(BBCC)| \right) = \\ &= \frac{1}{2} \text{ArcCosh} (\cosh^2 2a) = 2a - \log \sqrt{2} + 3e^{-4a} + o(e^{-6a}); \end{aligned} \quad (11)$$

And in the last case

$$\begin{aligned} \ell(\underline{\gamma_{[\Delta\nabla\Delta]}}) &= \frac{1}{4}\ell(\gamma_{(\Delta\nabla\Delta)}) = \frac{1}{2} \text{ArcCosh} \left(\frac{1}{2} |\text{tr}(B^{-1}CB^{-1}C)| \right) = \\ &= \frac{1}{2} \text{ArcCosh} \left(\frac{e^{4a} + e^{-4a}}{8} + \frac{e^{2a} + e^{-2a}}{2} - \frac{1}{4} \right) = 2a - \log 2 + 2e^{-2a} - 5e^{-4a} + o(e^{-4a}). \end{aligned} \quad (12)$$

■

In particular, we have the following corollary.

Corollary 1.

$$\ell(\underline{\gamma_{[\sigma_1\sigma_2\sigma_3]}}) = \begin{cases} 2a, & \text{if } \sigma_1 = \sigma_2 = \sigma_3; \\ 2a - \log \sqrt{2} + o(e^{-3a}), & \text{if } \sigma_1 = \sigma_2 \neq \sigma_3; \\ 2a - \log 2 - 2e^{-2a} + o(e^{-3a}), & \text{if } \sigma_1 = \sigma_3 \neq \sigma_2; \\ 2a - \log 2 + 2e^{-2a} + o(e^{-3a}), & \text{otherwise.} \end{cases}$$

Remark 1. This explains why the case $a = k \log 2$ is different. In particular, we see that this choice makes the length of short geodesics rationally dependent.

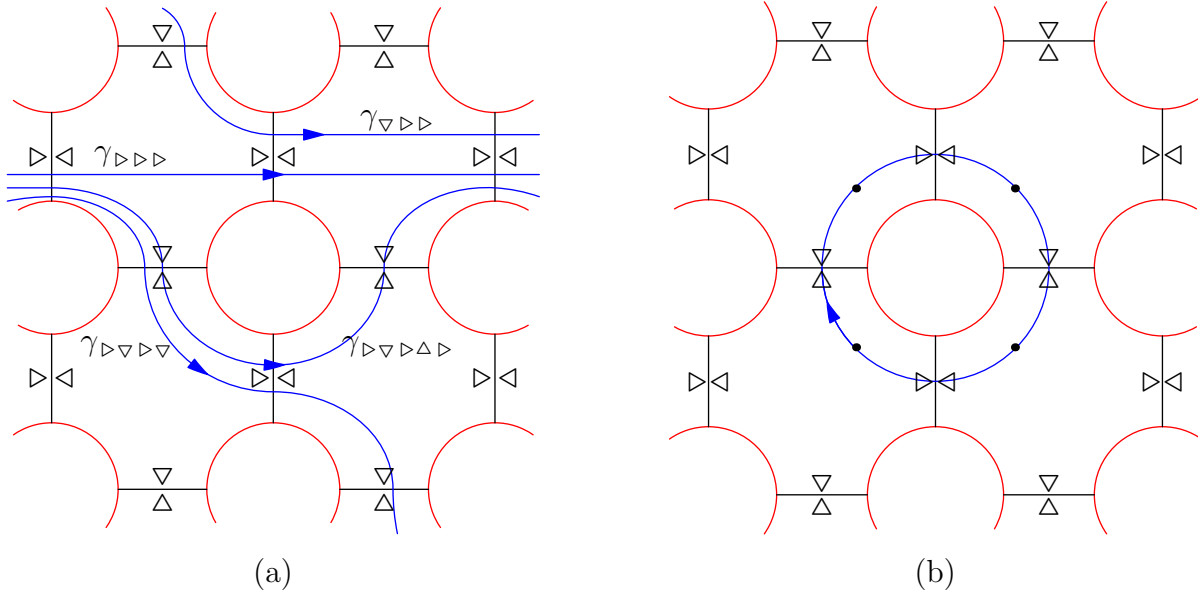


Figure 5: (a) Segments of geodesics lifted to the $\mathbb{Z} \times \mathbb{Z}$ holed plane, marked by subsequences of their cutting sequences, according to visible intersections. (b) The shortest closed geodesic among $\gamma_{\Delta\triangleright\nabla}$ corresponding to periodic sequence $(\Delta\triangleright\nabla\triangleleft)$ of period 4. The four marked points divide the geodesic into 4 equal segments: $\underline{\gamma_{[\Delta\triangleright\nabla]}}$, $\underline{\gamma_{[\triangleright\nabla\triangleleft]}}$, $\underline{\gamma_{[\nabla\triangleleft\Delta]}}$, and $\underline{\gamma_{[\triangleleft\Delta\triangleright]}}$.

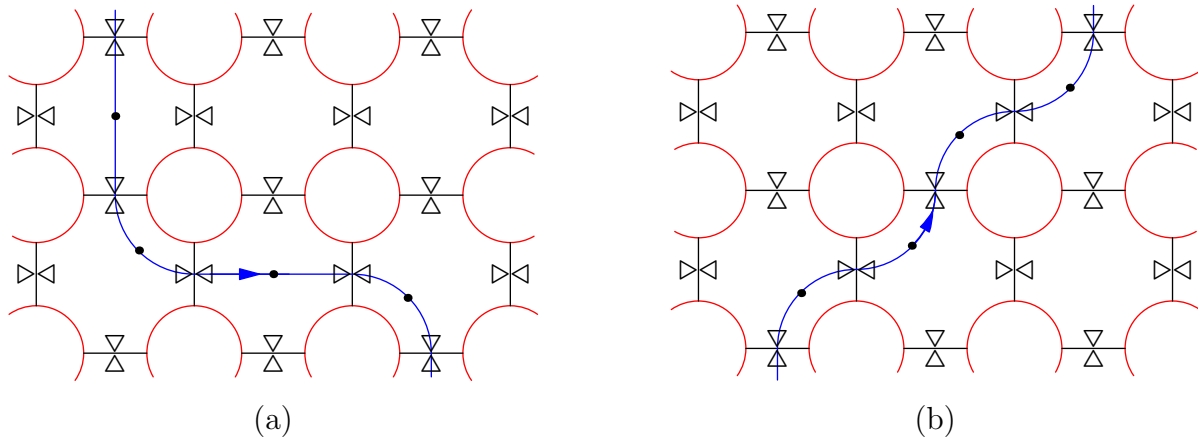


Figure 6: (a) The shortest closed geodesic among $\gamma_{\nabla\nabla\triangleright}$, corresponding to the periodic sequence $(\nabla\nabla\triangleright)$ of period 4. The four marked points divide the geodesic into 4 equal segments: $\underline{\gamma_{[\nabla\nabla\triangleright]}}$, $\underline{\gamma_{[\nabla\triangleright]}}$, $\underline{\gamma_{[\triangleright\nabla]}}$, and $\underline{\gamma_{[\nabla\nabla\triangleright]}}$. (b) The shortest closed geodesic among $\gamma_{\Delta\triangleright\Delta}$, corresponding to the periodic sequence $(\Delta\triangleright\Delta)$ of period 4. The four marked points divide the geodesic into 4 equal segments: $\underline{\gamma_{[\Delta\triangleright\Delta]}}$, $\underline{\gamma_{[\triangleright\Delta]}}$, $\underline{\gamma_{[\Delta\triangleright]}}$, and $\underline{\gamma_{[\triangleright\Delta]}}$.

We now apply the Corollary to compute the matrix $A(s)$ for $n = 2$. There are 12 subsequences of length 2 of the sequences from $\Sigma^{\mathbb{A}}$. We can enumerate them as follows $\sigma^1 = \Delta\Delta$, $\sigma^2 = \Delta\triangleright$, $\sigma^3 = \Delta\triangleleft$, $\sigma^4 = \triangleright\triangleright$, $\sigma^5 = \triangleright\Delta$, $\sigma^6 = \triangleright\nabla$, $\sigma^7 = \nabla\nabla$, $\sigma^8 = \nabla\triangleright$, $\sigma^9 = \nabla\triangleleft$, $\sigma^{10} = \triangleleft\triangleleft$, $\sigma^{11} = \triangleleft\Delta$, $\sigma^{12} = \triangleleft\nabla$. Then using definition (5) we may compute, for example

$$\begin{aligned} A_{1,1}(s) &= \exp(-s \cdot \ell(\gamma_{[\Delta\Delta\Delta]})) = \exp(-2as); \\ A_{2,4}(s) &= \exp(-s \cdot \ell(\gamma_{[\Delta\triangleright\triangleright]})) = \exp(-2as) \cdot \sqrt{2^s} \cdot \exp(-s \cdot o(e^{-3a})); \\ A_{2,5}(s) &= \exp(-s \cdot \ell(\gamma_{[\Delta\triangleright\Delta]})) = \exp(-2as) \cdot 2^s \cdot \exp(2e^{-2a}s) \cdot \exp(-s \cdot o(e^{-3a})); \\ A_{2,6}(s) &= \exp(-s \cdot \ell(\gamma_{[\Delta\triangleright\nabla]})) = \exp(-2as) \cdot 2^s \cdot \exp(-2e^{-2a}s) \cdot \exp(-s \cdot o(e^{-3a})); \end{aligned}$$

the other elements are similar. Observe that for values of s within the critical strip, $0 < \Re s < 0.2$, we have that $|\exp(-s \cdot o(e^{-3a})) - 1| \leq 2e^{-3a}$ is small for a sufficiently large. Introducing a shorthand notation

$$p_1(s) = \sqrt{2^s} \tag{13}$$

$$p_2(a, s) = 2^{s+1} \cosh(2se^{-2a}), \tag{14}$$

$$p_3(a, s) = 2^{s+1} \sinh(2se^{-2a}); \tag{15}$$

we may consider a matrix

$$P(s) = \begin{pmatrix} 1 & p_1 & p_1 & 0 & 0 & 0 & 0 & 0 & 0 & 0 & 0 & 0 \\ 0 & 0 & 0 & p_1 & \frac{p_2-p_3}{2} & \frac{p_2+p_3}{2} & 0 & 0 & 0 & 0 & 0 & 0 \\ 0 & 0 & 0 & 0 & 0 & 0 & 0 & 0 & 0 & p_1 & \frac{p_2-p_3}{2} & \frac{p_2+p_3}{2} \\ 0 & 0 & 0 & 1 & p_1 & p_1 & 0 & 0 & 0 & 0 & 0 & 0 \\ p_1 & \frac{p_2-p_3}{2} & \frac{p_2+p_3}{2} & 0 & 0 & 0 & 0 & 0 & 0 & 0 & 0 & 0 \\ 0 & 0 & 0 & 0 & 0 & 0 & p_1 & \frac{p_2-p_3}{2} & \frac{p_2+p_3}{2} & 0 & 0 & 0 \\ 0 & 0 & 0 & 0 & 0 & 0 & 1 & p_1 & p_1 & 0 & 0 & 0 \\ 0 & 0 & 0 & p_1 & \frac{p_2+p_3}{2} & \frac{p_2-p_3}{2} & 0 & 0 & 0 & 0 & 0 & 0 \\ 0 & 0 & 0 & 0 & 0 & 0 & 0 & 0 & 0 & p_1 & \frac{p_2+p_3}{2} & \frac{p_2-p_3}{2} \\ 0 & 0 & 0 & 0 & 0 & 0 & 0 & 0 & 0 & 1 & p_1 & p_1 \\ p_1 & \frac{p_2+p_3}{2} & \frac{p_2-p_3}{2} & 0 & 0 & 0 & 0 & 0 & 0 & 0 & 0 & 0 \\ 0 & 0 & 0 & 0 & 0 & 0 & p_1 & \frac{p_2+p_3}{2} & \frac{p_2-p_3}{2} & 0 & 0 & 0 \end{pmatrix}.$$

Then the matrix $A(s)$ can be considered as a small perturbation of $\exp(-2as)P(s)$. By Lemma from [7], the determinant $\det(I - A(s))$ approximates the Selberg zeta function. Since the matrices $\exp(-2as)P(s)$ and $A(s)$ are close, the determinant $\det(I - \exp(-2as)P(s))$ is an approximation to the zeta function, too. We see that the function $\det(I - \exp(-2as)P(s))$ is an exponential sum in s , and therefore an almost periodic function with modul $\langle a, \log 2, 2e^{-2a} \rangle$ if $a \notin \log 2\mathbb{Z}$ and $\langle \log 2, 4^{-k} \rangle$ otherwise. It follows from general theory of almost periodic functions

that its zeros is a point-periodic set in the sense of Krein–Levin. The simplicity of the matrix P allows us to get more information on exact location of the zeros of the determinant. Evidently, the matrix $\exp(-2as)P(s)$ has an eigenvalue 1 if and only if $\exp(2as)$ is an eigenvalue of $P(s)$. The eigenvalues of the matrix $P(s)$ have a closed form.

$$\lambda_{1,2} = \pm p_3 \tag{16}$$

$$\lambda_{3,4} = \frac{1}{2} \left(1 - p_2 \pm \sqrt{(p_2 + 1)^2 - 8p_1^2} \right) \tag{17}$$

$$\lambda_{5,6} = \frac{1}{2} \left(1 + p_2 \pm \sqrt{(p_2 - 1)^2 + 8p_1^2} \right) \tag{18}$$

Introducing a shorthand notation $\tilde{p}(p_1, p_2, p_3) = 9p_3 \cdot (3p_1^2 - p_2) - 1$ we write the remaining six eigenvalues as follows

$$\lambda_{7,8} = \frac{1}{3} \left(1 + \frac{3p_3p_2 - 1}{\sqrt[3]{\sqrt{\tilde{p}^2 - (3p_3p_2 - 1)^3 - \tilde{p}}}} + \sqrt[3]{\sqrt{\tilde{p}^2 - (3p_3p_2 - 1)^3 - \tilde{p}}} \right); \tag{19}$$

$$\lambda_{9,10} = \frac{1}{3} - \frac{i\sqrt{3} + 1}{6} \cdot \frac{3p_3p_2 - 1}{\sqrt[3]{\sqrt{\tilde{p}^2 - (3p_3p_2 - 1)^3 - \tilde{p}}}} + \frac{i\sqrt{3} - 1}{6} \cdot \sqrt[3]{\sqrt{\tilde{p}^2 - (3p_3p_2 - 1)^3 - \tilde{p}}}; \tag{20}$$

$$\lambda_{11,12} = \frac{1}{3} + \frac{i\sqrt{3} - 1}{6} \cdot \frac{3p_3p_2 - 1}{\sqrt[3]{\sqrt{\tilde{p}^2 - (3p_3p_2 - 1)^3 - \tilde{p}}}} - \frac{i\sqrt{3} + 1}{6} \cdot \sqrt[3]{\sqrt{\tilde{p}^2 - (3p_3p_2 - 1)^3 - \tilde{p}}}. \tag{21}$$

Summing up, we deduce the following

Proposition 1. *Any small zero of the zeta function $\zeta_{\mathbb{T}(a)}$ is close to a solution of one of the twelve equations*

$$\exp(2as) = \lambda_j(p_1(s), p_2(s), p_3(s)), \quad j = 1, \dots, 12, \tag{22}$$

where λ_k , $k = 1, \dots, 12$ are given by (16)–(21).

We omit the proof here. Figure 7 shows the small zeros of the zeta function along with the zeros of the determinant.

In the next section we discuss properties of solutions of equations (22), or in other words, zeros of the determinant $\det(I - \exp(-2as)P(s))$.

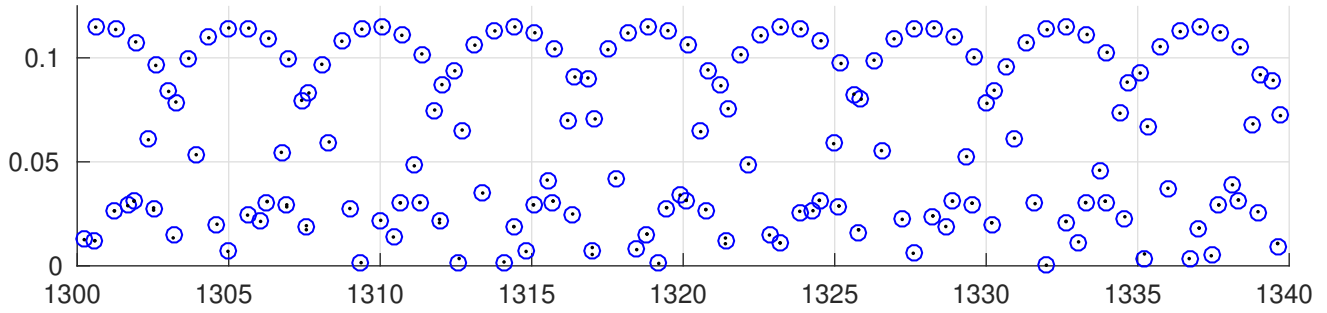
A.4 Zeros of the determinant

A.4.1 Solving $\lambda_{1,2}(s) = \exp 2as$.

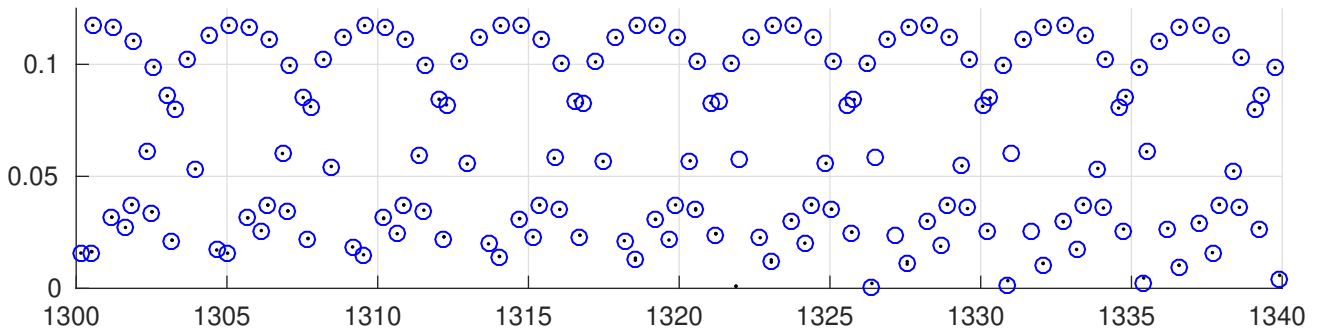
The first two eigenvalues have a simple form as functions of s and equation (22) gives us two equations:

$$\exp(2as) = \pm 2^{s+1} \sinh(2se^{-2a}). \tag{23}$$

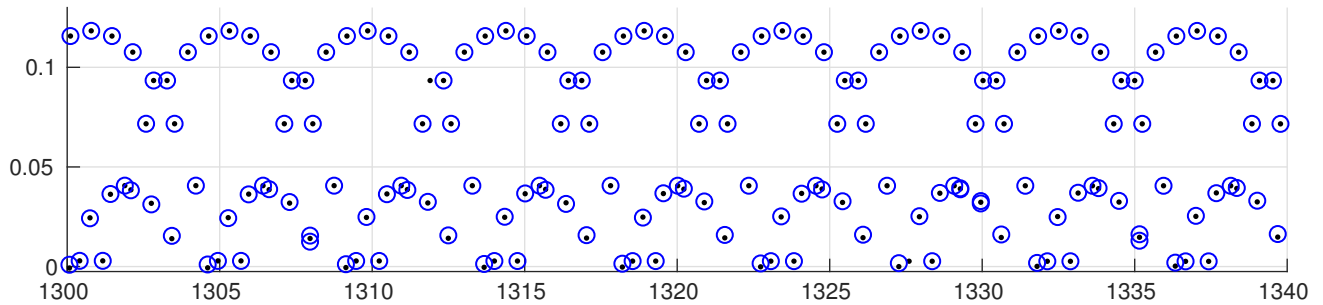
Figure 7: Zeros of the determinant $I - \exp(-2as)P(s)$ (circles) and zeros of the zeta function (dots) in a small part of the critical strip $1300 < \Im z < 1340$. In the cases we consider $\exp(\frac{3a}{2}) \approx 1400$.



(a) The case of $\mathring{\mathbb{T}}(10)$.



(b) The case of $\mathring{\mathbb{T}}(14 \log 2 + 0.05)$.



(c) The case of $\mathring{\mathbb{T}}(14 \log 2)$.

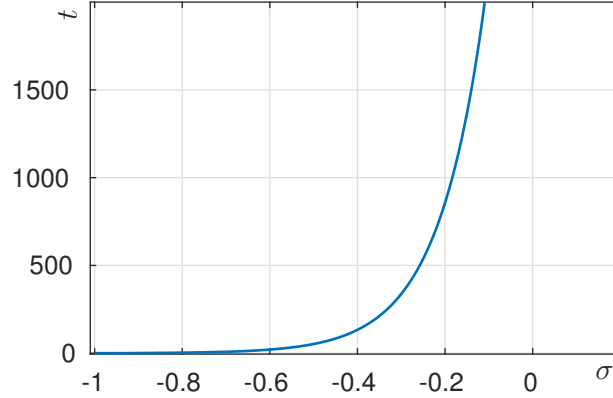


Figure 8: A plot of imaginary part $\Im(s) = t$ as a function of the real part $\Re(s) = \sigma$ as defined by (24). The zeros of the determinant $\det(I - A(s))$ defined by $\lambda_{1,2} = \exp(2as)$ are outside of the domain of approximation.

We may write $s = \sigma + it$ and use the equality between squares of the absolute values

$$|\exp((2a - \log 2)s)|^2 = |\sinh(2se^{-2a})|^2$$

to obtain

$$\exp((2a - \ln 2)2\sigma) = \exp(4\sigma e^{-2a}) + \exp(-4\sigma e^{-2a}) - 2\cos(4te^{-2a}),$$

which implies

$$t = \frac{e^{2a}}{4} \left(\pm \arccos \left(-\frac{1}{2} \exp((2a - \ln 2)2\sigma) + \cosh(4\sigma e^{-2a}) \right) + 2\pi k \right), \quad (24)$$

provided

$$\left| \frac{1}{2} \exp((2a - \ln 2)2\sigma) - \cosh(4\sigma e^{-2a}) \right| \leq 1.$$

Since for small σ we have that $\cosh(4\sigma e^{-2a}) = 1 + 4\sigma^2 e^{-4a} + o(e^{-6a})$, the above condition is valid provided $\sigma < \frac{\ln 2}{2a - \ln 2}$. However, for positive real part $\sigma > 0$ we have that imaginary part $t > \frac{1}{4}e^{2a}$, which is outside of the range of small zeros. Hence we have established the following

Lemma 3. *The first two eigenvalues (16) don't give any information on location of small zeros in positive half-plane.*

The equality (23) also implies the equality between arguments:

$$\arg(\exp((2a - \log 2)s)) = \arg(\sinh(2se^{-2a}))$$

We see that for $s = \sigma_0 + it$ the function $\arg(\sinh(2se^{-2a}))$ is monotone increasing and small, while $\arg(\exp((2a - \log 2)s))$ is changing rapidly. We therefore expect that solutions of (23)

with $|s| < e^{2a}$ belong to the curve given by (24) and the difference between imaginary parts of consecutive zeros is approximately $\frac{2\pi}{2a - \ln 2}$.

We now proceed to analyse the equations coming from the next four eigenvalues.

A.4.2 Solving $\lambda_{3,4}(s) = \exp 2as$ and $\lambda_{5,6}(s) = \exp 2as$.

The equations (22) read

$$2e^{2as} = 1 - 2^{s+1} \cosh(2se^{-2a}) \pm \sqrt{(2^{s+1} \cosh(2se^{-2a}) + 1)^2 - 2^{s+3}}, \quad (25)$$

$$2e^{2as} = 1 + 2^{s+1} \cosh(2se^{-2a}) \pm \sqrt{(2^{s+1} \cosh(2se^{-2a}) - 1)^2 + 2^{s+3}}, \quad (26)$$

which is equivalent to

$$e^{2as} (e^{2as} \cdot 2^{-s-1} - 2^{-s-1} + \cosh(2se^{-2a})) = \cosh(2se^{-2a}) - 1,$$

$$e^{2as} (e^{2as} \cdot 2^{-s-1} - 2^{-s-1} - \cosh(2se^{-2a})) = 1 - \cosh(2se^{-2a}).$$

The determinant $\det(I - \exp(-2as)P(s))$ approximates the zeta function on a part of the critical strip $0 < \Re(s) < \delta$, $0 < \Im(s) < e^{\frac{3a}{2}}$. We have the following asymptotic expansion for the right hand side:

$$\begin{aligned} |\cosh(2se^{-2a}) - 1| &\leq \sum_{j=1}^{\infty} |4^j e^{-4aj} s^{2j}| = \sum_{j=1}^{\infty} 4^j e^{-4aj} (\sigma^2 + t^2)^j \\ &\leq 4e^{-4a}(\sigma^2 + t^2) + 16e^{-8a}(\sigma^2 + t^2)^2. \end{aligned} \quad (27)$$

This allows us to deduce that zeros of the zeta function with imaginary part $\Im(s) = |t| \leq e^{\frac{3a}{2}} \approx 1800$ are close to solutions of the approximate equations

$$e^{2as} \cdot 2^{-s-1} - 2^{-s-1} + 1 = 0, \quad (28)$$

$$e^{2as} \cdot 2^{-s-1} - 2^{-s-1} - 1 = 0. \quad (29)$$

Evidently solutions of (28) and (29) should satisfy

$$|e^{2as}|^2 = |2^{s+1} - 1|^2 \text{ and } |2^{s+1}|^2 = |e^{2as} - 1|^2; \text{ or} \quad (30)$$

$$|e^{2as}|^2 = |2^{s+1} + 1|^2 \text{ and } |2^{s+1}|^2 = |e^{2as} - 1|^2. \quad (31)$$

and therefore belong to the intersections $\mathcal{T}_1 \cap \mathcal{T}_2$ of the of curves given by

$$\mathcal{T}_1 \stackrel{\text{def}}{=} \left\{ \sigma + it \mid \cos(2at) = \pm \frac{1 + e^{2a\sigma} - 4^{1+2\sigma}}{2e^{2a\sigma}} \right\} \quad (32)$$

$$\mathcal{T}_2 \stackrel{\text{def}}{=} \left\{ \sigma + it \mid \cos(t \log 2) = \pm \frac{4^{1+2\sigma} + 1 - e^{4a\sigma}}{4^{1+\sigma}} \right\} \quad (33)$$

We summarize our findings in the following

Lemma 4. *There exist a zero of the zeta function $\zeta_{\mathbb{H}(a)}$ in e^{-a} -neighbourhood of every **odd** element of the following subsequences of the points of intersection with $\Im z_n < e^{\frac{3a}{2}}$ (see plots in Figure 9)*

$$z_n = \sigma_n + it_n \text{ where } \cos(2at_n) = \frac{1 + e^{2a\sigma_n} - 4^{1+\sigma_n}}{2e^{2a\sigma_n}}, \quad \cos(t_n \log 2) = \frac{e^{4a\sigma_n} - 4^{1+\sigma_n} - 1}{2^{2+\sigma_n}} \text{ and } t_n < t_{n+1};$$

$$z_n = \sigma_n + it_n \text{ where } \cos(2at_n) = \frac{4^{1+2\sigma_n} - 1 - e^{2a\sigma_n}}{2e^{2a\sigma_n}}, \quad \cos(t_n \log 2) = \frac{e^{4a\sigma_n} - 4^{1+\sigma_n} - 1}{2^{2+\sigma_n}} \text{ and } t_n < t_{n+1}.$$

Corollary 2. *In the case $a \in \mathbb{N} \log 2$ solutions to this system belong to the straight lines $\Im z = \sigma = \text{const}$; moreover, the intersection of the zero set with any of this lines is a periodic set of period $\frac{2\pi}{\log 2}$. These lines correspond to seemingly straight lines we see in Figure 2(a). In the case $a \notin \mathbb{N} \log 2$ this no longer holds and we see a random structure as shown in Figure 2(c).*

A.4.3 Analysing $\lambda_{7,8}(s) = \exp(2as)$

Let us now consider the remaining eigenvalues $|\exp(2as)| = |\lambda_k(s)|$, $7 \leq k \leq 12$. The explicit expressions (19), (20) and (21) can be used to compute the curves where the zeros are located numerically. It turns out that equation (22) have solutions in the domain of approximation only for $k = 7, 8$. In Figure 10(a) we see a part of the curve defined by

$$\mathcal{T}_3 = \{s = \sigma + it \mid |\exp(2as)| = |\lambda_k(s)|\} \quad (34)$$

for $k = 7, 8$; Figures 10(b) and 10(c) show two pieces of the curve corresponding to $0 < \Im s < 20$ and $310 < \Im s < 340$ with zeros of the zeta function located there.

In attempt to find a transversal family of curves that would help to describe location of the zeros more precisely, we would like to study the polynomial

$$\prod_{j=7}^{12} (x - \lambda_j(s)) = \det(P(s) - xI) \cdot \prod_{j=1}^6 (x - \lambda_j(s))^{-1}.$$

By straightforward calculation we obtain

$$\prod_{j=7}^{12} (x - \lambda_j(s)) = (x^3 - x^2 + p_2 p_3 x + (2p_1^2 - p_2)p_3)^2 \quad (35)$$

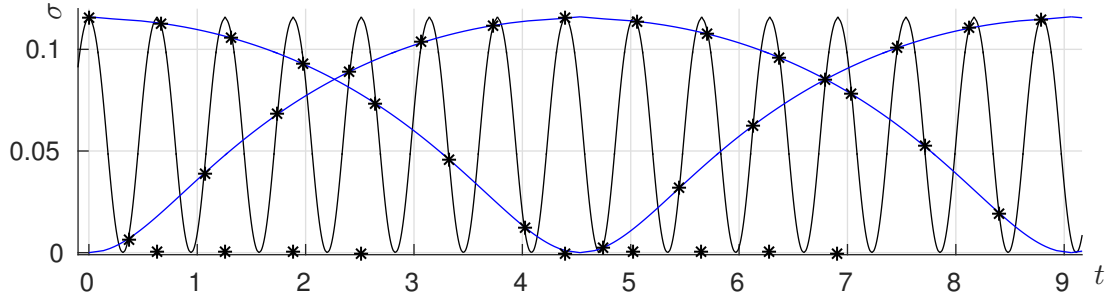
We would like to return to the original variable, s i.e. to reverse (13)–(15), taking into account that for $\Re(s) \ll 1$ we have that $\sinh(s) \approx i \sin(\Im(s))$ and $\cosh(s) \approx \cos(t)$:

$$p_1(s) \approx 2^{\frac{s}{2}}; \quad (36)$$

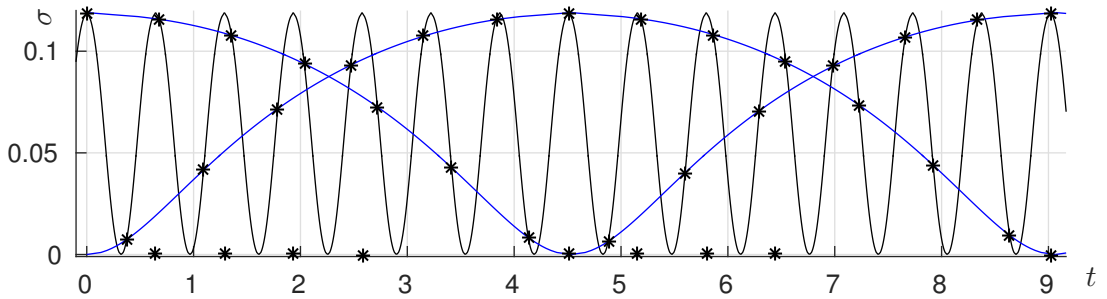
$$p_2(s) \approx 2^{s+1} \cos(2te^{-2a}); \quad (37)$$

$$p_3(s) \approx 2^{s+1} \sin(2te^{-2a}) \sqrt{-1}. \quad (38)$$

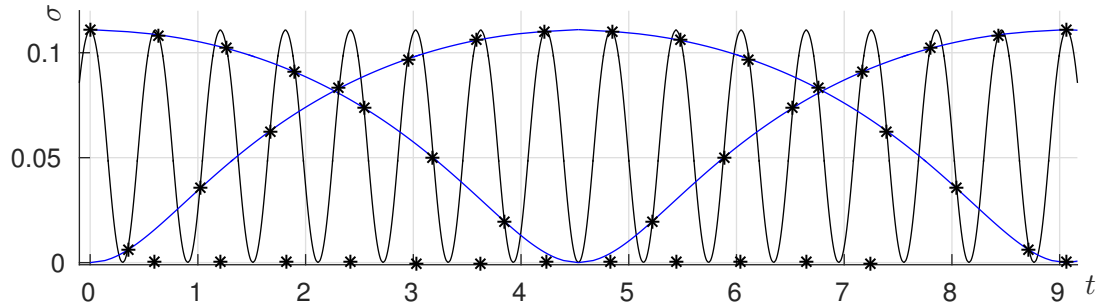
Figure 9: Families of curves \mathcal{T}_1 quickly oscillating with period $\frac{\pi}{a}$ and \mathcal{T}_2 slowly oscillating with period $\frac{2\pi}{\log 2}$ as defined by (32) and (33) and described in Lemma 4 and zeros of the 12th Taylor polynomial approximating the zeta function (stars). We see that the actual zeros occur very close to odd elements of the sequences of points of intersections. Zeros on imaginary axis correspond to solutions of $e^{2as} = \lambda_{7,8}(s)$.



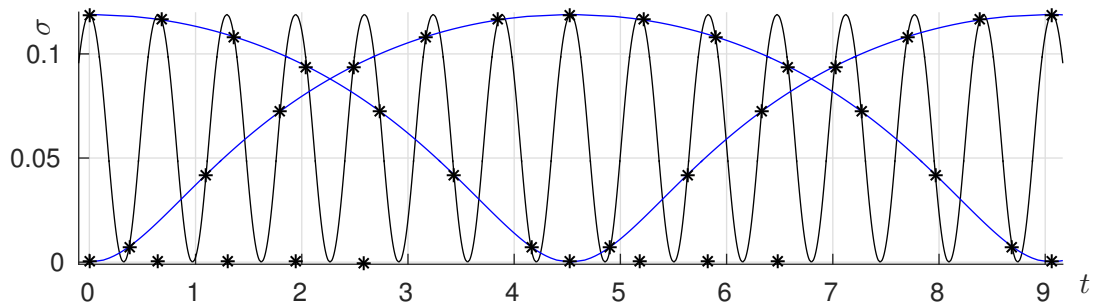
(a) Case $a = 10$. A part of the zero set from Figure 2(a).



(b) Case $a = 14 \log 2 + 0.05$. A part of the zero set from Figure 2(b).



(c) Case $a = 14 \log 2$. A part of the zero set from Figure 2(c).



(d) Case $a = 15 \log 2$. Together with the plot above they illustrate Corollary 2.

We obtain an approximation

$$\prod_{j=7}^{12} (x - \lambda_j(s)) \approx x^3 - x^2 + i2^{2s+1} (\sin(4e^{-2a}t)(x-1) + 2\sin(2e^{-2a}t)).$$

The latter implies

$$2^{4\sigma+2} = |2^{2s+1}|^2 = \left| \frac{(x^3 - x^2)}{(\sin(4e^{-2a}t)(x-1) + 2\sin(2e^{-2a}t))} \right|^2. \quad (39)$$

Substituting $x = \exp(2as)$ we solve the equation for $\cos(2at)$ and obtain the equality

$$\cos(2at) = \frac{e^{8a\sigma}(e^{4a\sigma} + 1) - 2^{4\sigma+2} (\sin^2(4e^{-2a}t)(e^{4a\sigma} + 1) - 2\sin(4e^{-2a}t) + 4\sin^2(2e^{-2a}t))}{2e^{2a\sigma} (2^{4\sigma+2}(\sin(4e^{-2a}t) - \sin^2(4e^{-2a}t)) + e^{8a\sigma})} \quad (40)$$

We see that although the right hand side depends on t , as t varies in any small interval of length $c \ll \exp(a)$, say $(nc, (n+1)c)$ the dependence on t is negligible, so we may consider a partition into intervals of length c and the curves defined by

$$\mathcal{T}_4 = \left\{ \sigma + it \mid \cos(2at) = \frac{e^{8a\sigma}(e^{4a\sigma+1}) - 2^{4\sigma+2} (\sin^2(4e^{-2a}nc)(e^{4a\sigma} + 1) - 2\sin(4e^{-2a}nc) + 4\sin^2(2e^{-2a}nc))}{2e^{2a\sigma} (2^{4\sigma+2}(\sin(4e^{-2a}nc) - \sin^2(4e^{-2a}nc)) + e^{8a\sigma})} \right\} \quad (41)$$

on the intervals $nc < t < (n+1)c$, $n \in \mathbb{Z}$.

Remark 2. The dependence of the right hand side on t is reflected in increasing amplitude of oscillations of the curve in Figure 10(a). It is possible to make further simplification of the right hand side of (41), using first order approximations $\sin(x) \approx x$ and $\cos(x) \approx 1$ for small x . This would lead to

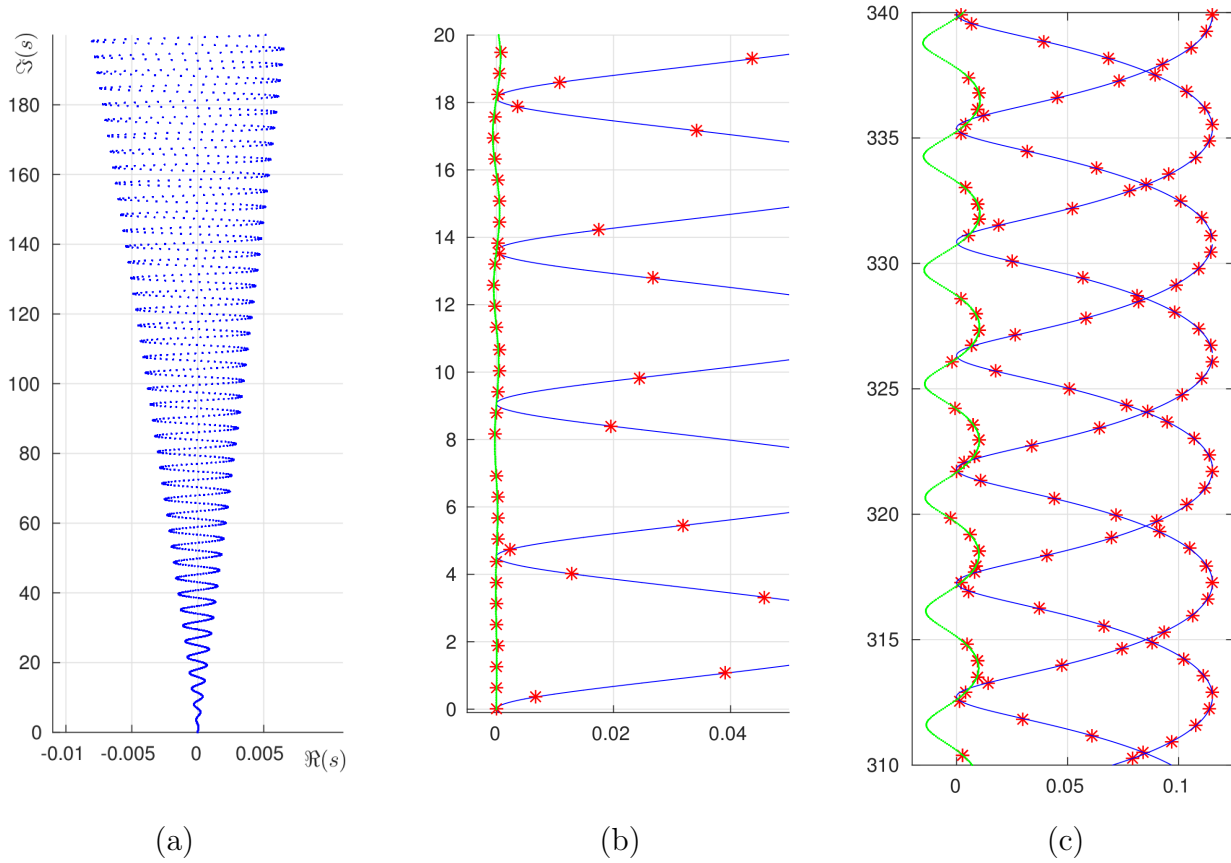
$$\mathcal{T}'_4 = \left\{ \sigma + it \mid \cos(2at) = \frac{e^{8a\sigma}(e^{4a\sigma} + 1) - 2^{4\sigma+5}e^{-2a}t(2e^{-2a}t(e^{4a\sigma} + 2) - 1)}{2e^{2a\sigma}(2^{4\sigma+4}e^{-2a}t(1 - 4e^{-2a}t) + e^{8a\sigma})} \right\}. \quad (42)$$

It is evident that the plot will be a quickly oscillating curve with period $\frac{\pi}{a}$ and increasing amplitude of oscillations.

We summarize our discussion in this section as follows.

Proposition 2. *Zeros of the zeta function in the critical strip with imaginary part $\Im s < e^a$ are e^{-a} -close either to the intersections $\mathcal{T}_1 \cap \mathcal{T}_2$, as described in Lemma 4 or to the intersections $\mathcal{T}_3 \cap \mathcal{T}_4$.*

Figure 10: Several plots showing the curve $|\exp(2as)| = |\lambda_{7,8}(s)|$. (a) General plot of the curve within the rectangle $-0.01 < \Re s < 0.01$, $0 < \Im s < 200$; (b) A part of the curve near the real axis $-0.005 < \Re s < 0.05$, $0 < \Im s < 20$, stars mark zeros of the zeta function, the oscillating curve in horizontal direction is \mathcal{T}_2 ; (c) The curve in the part of the critical strip $0 < \Re s < \delta$, $310 < \Im s < 340$, oscillating around imaginary axis. Stars mark zeros of the zeta function. The second oscillating curve is \mathcal{T}_2 .



References

- [1] Beardon, A. F. The geometry of discrete groups. Corrected reprint of the 1983 original. Graduate Texts in Mathematics, 91. Springer-Verlag, New York, 1995.
- [2] Borthwick, D. Distribution of resonances for hyperbolic surfaces. *Exp. Math.* 23 (2014), no. 1, 25–45.
- [3] Borthwick, D. and Weich, T. Symmetry reduction of holomorphic iterated function schemes and factorization of Selberg zeta functions, *J. Spectral Theory*, 6 (2016) 267–329.
- [4] Borthwick, D, Dyatlov, S., and Weich T. Improved fractal Weyl bounds for hyperbolic manifolds
- [5] Buser, P. and Semmler, K.-D. The geometry and spectrum of the one holed torus. *Commentarii mathematici Helvetici* 63.2 (1988): 259–274
- [6] McMullen, C. T. Hausdorff dimension and conformal dynamics. III. Computation of dimension. *Amer. J. Math.* 120 (1998), no. 4, 691–721.
- [7] Pollicott, M. and Vytnova, P. Zeros of the Selberg zeta function for symmetric infinite area hyperbolic surfaces. Preprint.
- [8] Series, C. The geometry of Markoff numbers. *Math. Intelligencer* 7 (1985), 20–29.
- [9] Weich, T. Resonance chains and geometric limits on Schottky surfaces. *Comm. Math. Phys.* 337 (2015), no. 2, 727–765.